IEEE Access
Multidisciplinary ⋮ Rapid Review ⋮ Open Access Journal

Received 9 January 2024, accepted 11 February 2024, date of publication 14 February 2024, date of current version 27 February 2024.

Digital Object Identifier 10.1109/ACCESS.2024.3366454

RESEARCH ARTICLE

A Three-Stage MCDM and Extended Longest Path Algorithm for the Satellite Image Acquisition Scheduling Problem

ALEX ELKJÆR VASEGAARD[1], MATHIEU PICARD[2], PETER NIELSEN[1], AND SUBRATA SAHA[3]

[1]Department of Materials and Production, Aalborg University, 9220 Aalborg, Denmark
[2]Airbus Defence and Space, 31555 Toulouse, France
[3]Department of Basic and Applied Science, University of Engineering and Management, Kolkata 700160, India

Corresponding author: Alex Elkjær Vasegaard (aev@mp.aau.dk)

This work was supported in part by Airbus Defense & Space.

ABSTRACT For a constellation of agile Earth Observation Satellites (EOS), efficiently scheduling image acquisitions presents a complex decision-making challenge characterized by balancing a multitude of qualitative and quantitative preferences on the imaging requests while considering a high number of operational and temporal constraints. Current research predominantly focuses on the scheduling aspect, often neglecting the fuzzy multi-objective nature of the problem and the near real-time computation requirement. This study proposes an innovative three-stage solution method. Initially, an a priori multi-criteria scoring approach, based on the ELECTRE-III method's fuzzy pairwise evaluation, is employed to value each potential imaging attempt, addressing the gap in comprehensive pre-scheduling valuation. The problem is then redefined as a Longest Path Problem in a Directed Acyclic Graph with Interdependent and Allowed Nodes (DAG-IAN). This re-conceptualization accommodates unique multi-satellite operational needs and imaging techniques such as stereo and strip acquisitions. We introduce the Extended Longest Path Algorithm (ELPA) for this purpose, which emerges as a novel solution mechanism. The final stage is a decision support system designed to guide decision-makers through the satellite operation's intricate trade-offs, facilitating iterative enhancements and a deeper understanding of the conflicting objectives through a weight space analysis and a significance test. Our approach not only demonstrates high adaptability and explainability but also shows computationally efficient performance. In smaller problem scenarios, the ELPA closely approximates exact methods while significantly outperforming other approaches in large-scale applications. The research advances state of the art by offering an intuitive, customizable, and scalable framework in the preference integration aspect of the Satellite Image Acquisition Scheduling Problem.

INDEX TERMS Satellite image acquisition scheduling problem, agile earth observation satellites, multi-criteria decision making, directed acyclic graph, longest path algorithm, weight space analysis.

I. INTRODUCTION

Selecting the optimal set of image acquisitions for a constellation of agile high-resolution Earth Observation Satellites (EOSs) is a complex combinatorial problem incorporating a high number of operational constraints and qualitative preferences [1], [2]. In the Satellite Image Acquisition Scheduling Problem (SIASP), multiple preference conflicts exist, e.g., the trade-off between obtaining as many high-priority images or high-quality acquisitions as possible. Furthermore, as the last delivery date nears, the sun elevation lowers, or other criteria affecting quality decrease, the intricate priority structure between any two attempts changes dynamically. A low-priority image request with a due delivery date can be preferred over a higher-priority image request if they are conflicting, as the alternative otherwise is a lost customer.

The associate editor coordinating the review of this manuscript and approving it for publication was Bijoy Chand Chatterjee.

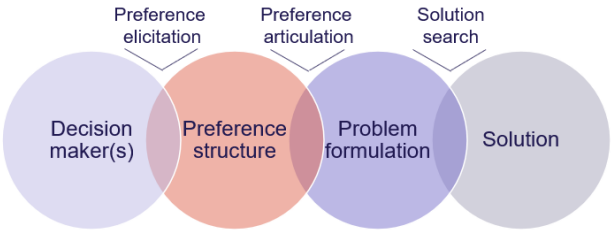

FIGURE 1. A holistic illustration of the procedure behind an automated decision-making scheme. In order for a proper automatic decision process to take place, the four domains should overlap as much as possible, meaning the preference structure reflects the decision maker (DM), the problem formulation integrates the preference structure, and the solution maximizes the objectives through the problem formulation. See the work of A. E. Vasegaard [7] for a detailed discussion on the automatic decision procedure.

EOSs has several advantages relative to other image acquisition approaches, e.g., large acquisition capability in a relatively short time, worldwide coverage, high revisit frequency enabling repeated imagery, increasing accessibility to space, and unlimited airspace borders. Simultaneously, the growing technical capabilities of satellites such as agility, memory, communication, or imaging types (passive or active imagery; s.a., panchromatic, multi-spectral, pan-sharpened, hyper-spectral, and microwave radiometry; or synthetic aperture radar, Lidar, radar altimetry, GNSS-R, and radar scatterometry, respectively) allow for information retrieval of multiple different objectives, whether it stems from a purpose of global monitoring of the environment, earth mapping, urban development, disaster management, agriculture, maritime surveillance, or Intelligence, Surveillance, and Reconnaissance (ISR) for defense. As a result, the total number of EOSs launched has increased extensively and reached 1,184 by January 2023, according to the database at the Union of Concerned Scientists [3]. Consequently, the high demand for EOS imagery has led to increased interest from research communities in the EOS scheduling problem, which, when omitting the ground station communication, formally is denoted by the Agile EOS Scheduling problem (AEOSSP) or the Satellite Image Acquisition Scheduling Problem (SIASP) [4]. The mathematical problem is equivalent to the satellite broadcast scheduling problem [5] and even the space telescope observation scheduling problem [6].

In multi-objective (MO) optimization problems with real-time execution requirements, adding a decision maker (DM) to evaluate a high-dimensional Pareto front in operation is not feasible, so the question is how to deploy a preference structure, weight setting, or goal such that no matter the scenario, the DMs will always be satisfied with the solution. To do this, we must not only focus on objectives but also consider criteria associated with the image attempts. Hence, we seek an automated decision-making scheme to be implemented in this problem domain, omitting the regular a posteriori approaches and investigating those that a priori integrates preferences. In doing so, we want to ensure that the DM has as much control over each domain in the automated decision-making scheme presented in Figure 1.

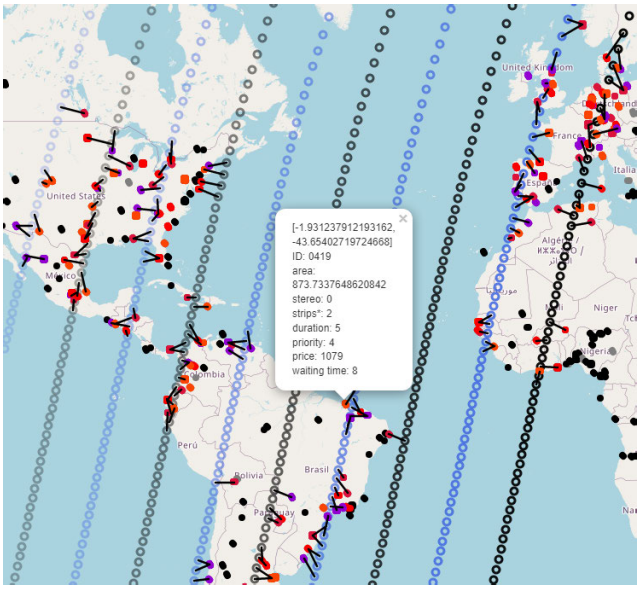

FIGURE 2. A map representation of a generated problem scenario and the corresponding solution. Note the colors of the requests convey information to the DM of either qualitative, political, or operational character. E.g., an image request from a high priority customer is colored purple. See the source codes for the details on the scenario generator.

For the SIASP, the DM faces the great challenge of balancing the multiple criteria affecting the decision process such that it aligns with the preferences of all stakeholders of the satellite operation while resulting in the highest number of high-quality acquisitions under the uncertainty of cloud cover, as well as satisfying operational constraints like maneuverability, energy, memory, reachability, etc. This is, however, a very difficult task, as the stakeholders of the satellite operation cover the investors, employees, customers, executive leadership, and even the greater community. When utilizing a posteriori MO approach, the DM still faces complicated comparative tasks in selecting a solution from the Pareto front, especially when many objectives are integrated in the evaluation. Similarly, when using standard a priori approaches, there is difficulty in defining a fitting preference structure. It is, for example, challenging to state the direct preference where a high-priority image attempt with cloud coverage lower than 10 % must be preferred over any other image attempt through a weight setting scheme. In addition, not understanding the combined effect of all criteria when defining rules in the scoring procedure can lead to unintentional bias.

Therefore, unlike the existing approaches, we formulate and analyze the SIASP through a three-stage solution approach that combines a customizable a priori decision framework with an explainable a posteriori tuning framework. Firstly, a multi-criteria scoring approach that builds on the MCDM method, ELECTRE-III, is utilized to value each image attempt. Secondly, due to the complexity of the multi-SIASP, we formulate the problem as a longest path problem in a Directed Acyclic Graph with Interdependent and Allowed Nodes (DAG-IAN). The graph-based representation of the

satellite network integrates the multi-satellite framework, stereo, and strip acquisition characteristics. We employ the Extended Longest Path Algorithm (ELPA) to obtain a solution. Thirdly, a Weight Space Analysis (WSA) is conducted to explain the weight setting of the scoring procedure, while a significance test allows the DM to adjust their preference structure s.t. it follows the quality objectives, priority structure, and behavioral aspects. We perform an extensive simulation study to present the expected outcomes of the weight space. The overall solution approach for the SIASP is visualized in Figure 3.

This paper is organized as follows; In Section II, the research works on MO optimization and the SIASP is briefly reviewed; Section III explains the model formulation, utilized methods, performance comparison, as well as the simulation procedure, WSA, and the significance test; Section IV discusses the findings and showcases the utility and application of the system from a managerial perspective, as well as its relevance for other problem domains; Section V concludes on the findings.

II. RELATED WORKS

Generally, the SIASP is addressed through a two-phase solution approach, i.e., a pre-processing segment and scheduling of candidate attempts with an intrinsic scoring of each attempt [2], [8], [9]. The pre-processing conducts a discretization of the satellite paths, establishes all feasible attempts based on satellite reachability, decomposes feasible customer requests, and computes all relevant criteria information on each attempt. The pre-processing is often trivial and specific to the solution approach; it is often neglected. The scoring procedure aligns the expected qualitative value of each attempt and the value assigned from the satellite operation's internal priority structure but is often diminished by only representing a single objective, e.g., maximizing expected number of images. In general, the majority of the SIASP literature focuses on the scheduling procedure and omits the managerial perspective of integrating preferences [10]. However, in the last couple of years, the literature has presented a plethora of multi-objective optimization approaches [11].

When considering multiple objectives and integrating DM preferences, the literature distinguishes between a priori, a posteriori, or interactive methods [12], in integrating the preferences before, after, or during the solution search, respectively. On the a posteriori side, various methods have been investigated to showcase the applicability [13], [14], [15]. In the works by Niu et al. [14], the multi-objective genetic algorithm, NSGA-II, was applied for rapid response to natural disasters. The general consensus seems to be that the SIASP is a many-objective problem. Therefore, regular a posteriori approaches are not applicable unless a high number of objectives are omitted; otherwise, a high-dimensional Pareto front must be obtained and evaluated, which is computationally expensive and often confusing for DMs. On the a priori side, and due to the many-objective aspect of the problem, an objective function combining multiple viewpoints is often seen constructed with various levels of systematic reasoning [10], [11]. This could be as a customized reward function combining quality and the significance of a polygon [2], [16], a value function representing the expected value of profits executed under uncertainties of clouds [17], a function representing the "value of information" combining nominal value and profits [18], or a utility-based function [19], [20]. Additionally, a single objective is often picked to represent a simplified version of the DM's preferences. This could be profit [9], [21], [22], [23], marginal profit [8], gain of polygons [24], or total attitude maneuvering time [25], and sometimes, the issue of defining an objective is completely omitted [26], [27]. Only a few works have actually implemented a systematic approach to integrate preferences a priori [28], [29], [30]. Notably, Hierarchical approaches, which iteratively obtain a solution given one objective and then constrain the solution space have shown great promise for real-time scheduling [31]. Similarly, the works by Wang et al. [30] utilize a bargaining mechanism relying on the theory of Nash equilibrium to evaluate a bi-objective framework and arrive at a compromise solution. In the paper by Baek et al. [32], a customizable weighted scoring approach implementing an array of parameters is presented in the context of a GUI. Preferences can also be introduced through an interactive selection stage [19], [33], but as the real-time requirements and size of the problem scenarios increase, so does the difficulty of the decision process, which will leave it impossible for the DM to manage every selection process.

Because of the issue in integrating preferences, combined versions of a posteriori, interactive, and a priori approaches have recently started appearing. The work by Li et al. [34] showed great promise as the preference-based algorithms t-NSGA-III are compared with other state-of-the-art MOEAs. An improved NSGA-III also showcased great results in integrating both a priori and a posteriori preferences in the satellite scheduling [35]. However, all this work still relies on the a posteriori integration of a DM in operation, which bypasses the possibility of real-time execution. The solution approach of this paper continues this quest by presenting a framework where operational preferences are integrated a priori but tuned a posteriori.

III. SOLUTION APPROACH

In the SIASP, a large set of decisions govern the outcome, e.g., how the intricate priority of customers relates to the physical quality of imaging attempts. Additionally, the decision environment changes regularly due to new regulations, new priority structures of the satellite operation, etc. As a proper preference structure is complex to define, some decisions and trade-offs are introduced through hierarchical scheduling or hard constraints to handle differently prioritized customer requests. However, the proper preference structure is often neglected or simplified when decisions are imposed by constraints, as these decisions are scenario-specific. Ultimately

the valuation of requests imposed by the defined priority structure should reflect three aspects of the decision making in the SIASP:

1) *The political agenda* reflects the intricate priority structure of customers relative to other customers
2) *The qualitative agenda* is imposed on the criteria set to maximize the quality of the acquired images
3) *The operational agenda* convey the changing value of attempts relative to the resoluteness of time until expiration of requests, the uncertainty of cloud coverage, willingness to complete requests, multi-strip, or stereo request completion

Note cross-agenda decisions also exist, e.g., the value of a high-priority, low-quality acquisition with high uncertainty relative to low priority, high-quality acquisition with low uncertainty. This paper introduces a solution approach where the different agendas are incorporated in the scoring procedure.

A. MODEL FRAMEWORK

To generate a problem scenario for the SIASP, three important types of information must be attained: **customer-specific information** (e.g., request location, type, area, customer type), **satellite-specific information** (e.g., satellite orbit, planning horizon, maximum off-nadir angle, slew-speed, memory, or battery capacity), **intermediate information of satellite and customer** (e.g., feasible acquisition attempts and corresponding forecasted cloud cover, uncertainty, or depointing angle). An example of a generated problem scenario can be seen in Figure 2. See the source codes for the details on the scenario generator.

The customer-specific information focuses mainly on the data generation and is provided in detail in the Supplementary file S2. Generating customer requests located worldwide allows for experimentation of the scheduling procedure over longer periods, ultimately enabling the DM to understand the long-term effects of deciding between acquiring a request on different orbits while simultaneously scheduling other acquisitions.

The satellite-specific information is a multitude of mostly fixed data sources, e.g., the planning horizon from UTC 09:40 to 17:40 at the 26*th* of July 2022 for the two satellites, SPOT 6 and 7. We found their reference orbits through the Two-Line-Element set (TLEs) obtained from www.celestrak.com. Note we discretize the satellite paths given a temporal resolution variable τ, which indicates the satellite's position being considered for every τ seconds. The lower the resolution τ, the closer the solution will be to the solution of the continuous version. The size of the problem scenario will likewise increase when τ is increased. Additionally, we assume slew-speed to be constant and 2^o per sec [36]. A feasible attempt follows user-given threshold specifications of off-nadir angle relative to the satellite, sun-elevation angle, forecasted cloud coverage, and operational constraints.

The intermediate information of satellite and customer requests refers to all the relevant information deduced from knowing a satellite's position and the location of a customer's request. That is, incidence angle, sun elevation, cloud cover forecasts for the request, and uncertainty of that forecast. The computation details for **the intermediate information** can be found in the supplementary file of Section S-II.

The pre-processing computes the data frame P representing all feasible attempts and the relevant criteria for the particular problem scenario. See Table S1 for an example of a P data frame.

B. DIRECTED ACYCLIC GRAPH WITH INTERDEPENDENT AND ALLOWED NODES (DAG-IAN)

To model the decisions of the SIASP, we introduce the DAG-IAN. A general, DAG is a set of nodes connected by directed edges without the possibility of cycles, see Figs. 4 and 5 for an example of a SIASP and the corresponding DAG.

In the case of the DAG in Figure 5, a node represents an imaging attempt of a specific request. Some attempts acquire the same request, and as we have to ensure the stereo and strip constraint, we denote a set of nodes representing the same request as interdependent nodes. That is, a subset of the DAG where a maximum number of nodes from that set can be acquired. Similarly, some attempts are stereo attempts meaning they have to be acquired together. This adds a further constraint on which subsets from the DAG that must be acquired together. We denote any set of nodes with such characteristics as allowed nodes.

$$G[i,j] = \begin{bmatrix} 0 & 1 & 1 & 1 & 1 & 1 & 1 & 1 & 1 & 1 \\ & 0 & 1 & 1 & 1 & 1 & 1 & 1 & 1 & 1 \\ & & 0 & 0 & 1 & 1 & 1 & 1 & 1 & 1 \\ & & & 0 & 1 & 1 & 1 & 1 & 1 & 1 \\ & & & & 0 & 1 & 1 & 1 & 1 & 1 \\ & & & & & 0 & 1 & 1 & 1 & 1 \\ & & & & & & 0 & 0 & 0 & 1 \\ & & & & & & & 0 & 0 & 1 \\ & & & & & & & & 0 & 1 \\ & & & & & & & & & 0 \end{bmatrix},$$

$$B[r,i] = \begin{bmatrix} 1 & 0 & 0 & 0 & 1 & 0 & 0 & 0 & 0 & 0 \\ 0 & 1 & 1 & 0 & 0 & 1 & 1 & 0 & 0 & 0 \\ 0 & 0 & 0 & 1 & 0 & 0 & 0 & 1 & 1 & 1 \end{bmatrix},$$

$$b[r] = \begin{bmatrix} 1 \\ 2 \\ 2 \end{bmatrix},$$

$$A[s,i] = \begin{bmatrix} 0 & 0 & 0 & 1 & 0 & 0 & 0 & 1 & 0 & 0 \\ 0 & 0 & 0 & 0 & 0 & 0 & 0 & 0 & 1 & 1 \end{bmatrix},$$

$$w[i] = \begin{bmatrix} 1 & 1 & 2 & 3 & 2 & 2 & 2 & 2 & 2 & 3 \end{bmatrix}$$

The longest path in a DAG representation of a satellite network will yield the schedule that includes the image acquisitions that maximize the stated objective function. However, as the solution space is constrained by interdependent nodes and allowed nodes, such a path is not necessarily valid.

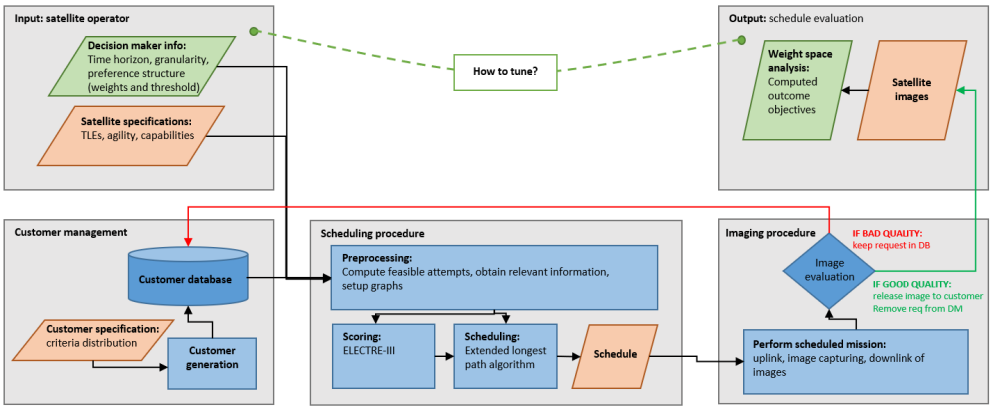

FIGURE 3. A holistic illustration of the solution procedure for the SIASP. The WSA seeks to investigate the relationship between the input and output of the system. Note the solution approach operates around the customer management scheme. Optimally, the entire solution procedure is automated, and adjustments are only made according to recommendations from the WSA.

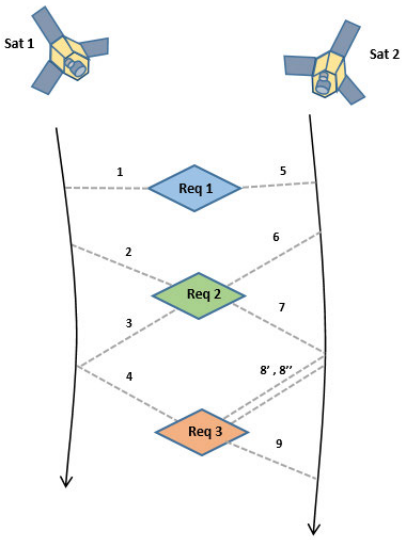

FIGURE 4. An example of a network representation for some arbitrary SIASP scenario. The specific scenario characteristics in terms of maneuverability, stereo attempt pairs, strip attempts, strip request type, and score are shown in the matrices G, A, B, b, and w. Note that request 1 is a regular request (a single acquisition must be made), request 2 is a strip request (two different acquisitions), and request 3 is a stereo request. Also, in this example, it is assumed that the two sets of attempts {4, 8} and {8, 9} create a complete stereo request acquisition, and it is, therefore, necessary to replicate attempt 8, which is why 8′ and 8″ are present.

By topologically sorting P and consequently the adjacency matrix G (order in which attempts appear) by first satellite and second time, the adjacency matrix (feasible maneuvers) is upper triangular. Ultimately, this permits G to represent a DAG-IAN constituting all feasible solutions with the interdependent and allowed nodes represented by the matrices B and A, respectively, and the maximum number of interdependent nodes by b, and the abstracted length illustrated by the vector w.

C. MODEL FORMULATION

We introduce the following operational constraints on the scheduling procedure:

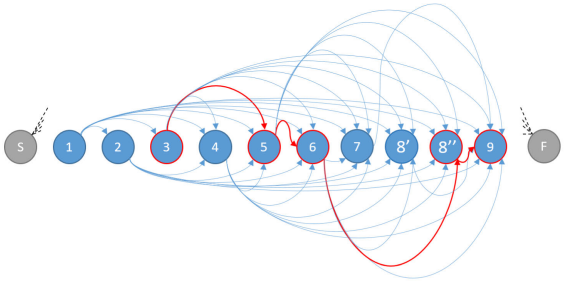

FIGURE 5. The SIASP scenario presented in Figure 4 represented as a DAG. The interdependencies and allowed nodes characteristics, which distinguish it as the DAG-IAN, are indicated by matrix B and A. Note the start and finish nodes are not necessary for the ELPA to work.

1) The payload of each satellite can only perform one task/request at a time [2].
2) Maneuvering time and acquisition duration make a set of attempts infeasible, i.e., some attempts cannot be performed sequentially if there is not enough time for maneuvering the attitude of the satellite.
3) A request must only be acquired once within the time horizon.
4) Requests too large to be acquired in one acquisition are segmented into multiple strips, jointly representing the full request [2].
5) We consider two types of requests: mono, where each area is acquired once; and stereo, where each area must be acquired twice, but from different angles (convergence angle between 15^o to 20^o) [13].
6) Satellites have limited memory and energy, constraining the schedule. [25].
7) Attempts must be initiated only if conditions are within some specified quality thresholds (max. off-nadir angle of 30^o, min. sun elevation of 15^o, max. forecasted cloud cover of 60% [36]).

Consequently, the problem can be formulated as a discrete multi-objective optimization problem with each feasible imaging attempt as an element in a binary decision variable x_i. If $x_i = 1$, the ith feasible attempt is acquired, and $x_i =$

0 otherwise. Correspondingly, in the scheduling procedure, we want to maximize the following objective function:

$$\max_{x\in X} F_\theta(x) = \max_{x\in X} g(f_1(x), f_2(x), \ldots, f_n(x), \theta) \quad (1)$$

$$= \max_{x\in X} \sum_{i\in N} c_i x_i \quad (2)$$

where N represents the total number of feasible attempts within the planning horizon, f_n is the nth objective function in the optimization problem, and c_i represents the corresponding non-negative value of the ith attempt when the a priori preferences, expressed by the parameter configuration θ regarding all objectives, are considered by the DM. Additionally, the function $F(.)$ is consequently a composite function $(g \circ \{f_1, f_2, \ldots, f_n\})(x)$, where the $g(.)$ function is the mapping of preferences towards all objectives. This assumes that we a priori know the preferences of the DM and the behavior of the Pareto front. Practically, creating a preference structure and mapping that accurately mirrors the decision maker's preferences is challenging, as the landscape of the Pareto front is unknown until optimization starts. It is therefore important to include a tuning procedure to align the DM's expectations with the outcome. This involves utilizing a system for decision support, which aids in fine-tuning the parameters based on DM feedback and preferences. This is described in detail in Section III-H.

The score, c_i, is computed through the ELECTRE-III approach, which is based on the concept of outranking. In this method, alternatives are compared pairwise across multiple criteria. The core intuition is to establish the extent to which one alternative is at least as good as another, considering all criteria. The scoring involves two main elements: concordance, which measures the degree of dominance of one alternative over another, and discordance, which assesses the extent of inferiority in certain criteria. This dual assessment helps in capturing the nuances of preference, particularly in cases where alternatives excel in different criteria. Consequently, the final score reflects a balance between these competing factors. See the Supplementary file S-I for an extensive explanation of the scoring method [28], [37], [38].

In extension to this, the set of constraints indicating the feasible region X can be formulated as:

1) Incorporating the maneuvering feasibility of the schedule involves considering the satellite's time consumption for maneuvering between two consecutive attempts and the acquisition duration of the former attempt. If the time consumption for the particular maneuver between two attempts for the same satellite exceeds the available time, this maneuver is infeasible.

$$\forall\{i, j\} : G_{i,j} = 0 \Rightarrow x_i + x_j \leq 1 \quad (3)$$

Here, the binary matrix G represents all such feasible pairs of attempts, thus being the adjacency matrix for the DAG-IAN. Note that G should be an upper triangular matrix, as P is ordered with respect to satellites and time in that order.

$$G_{i,j} = \begin{cases} 0 & \text{if } T^{man}_{i\mapsto j} + T^{acq}_i < t^{clock}_j - t^{clock}_i \\ & \quad \wedge \text{sat(i)} = \text{sat(j)} \\ 1 & \text{otherwise} \end{cases} \quad (4)$$

where the maneuvering duration, $T^{man}_{i\mapsto j}$ is computed based on the rotational speed of the satellite platform and the angle between the two vectors representing the line of sight of the satellite for the two acquisitions i and j in P. T^{acq}_i is the acquisition duration for i'th attempt, and t^{clock}_i is the starting time of acquisition i. The function sat(.) returns the satellite ID of the i'th attempt. Naturally, a maneuver can only be infeasible if it is performed by the same satellite.

2) A request can only be acquired multiple times if the additional acquisitions are due to the request being a multi-strip or stereo request. A specific number of each set of interdependent nodes can be included in the longest path.

$$\sum_{i\in N} B_{r,i} x_i \leq b_r \quad \forall r \in \{1, \ldots, R\} \quad (5)$$

where $B_{r,i}$ is a binary representation of every set r of unique attempts, and b_r is the upper limit for the number of acquisitions for that unique request. Note that R is the number of unique requests in P.

$$B_{r,i} = \begin{cases} 1 & \text{if id(i)} = \text{Uid}(r) \\ 0 & \text{otherwise} \end{cases} \quad (6)$$

where the functions id(.) and Uid(.) represent the request ID and enumerated unique request ID in P, respectively.

3) Some attempts represent stereo requests, which can only be acquired together in specific pairs to complete a request. That is, only specific pairs of these interdependent nodes are allowed together.

$$\sum_{i\in N} A_{s,i} x_i = \{0, 2\} \quad \forall s \in \{1, \ldots, S\} \quad (7)$$

The binary matrix A represents any allowed pair s of attempts that jointly represent a complete stereo request. S is the number of unique pairs of attempts completing a stereo request.

$$A_{s,i} = \begin{cases} 1 & \text{if id(i)} = \mathit{ID\_allowable}(s) \\ 0 & \text{otherwise} \end{cases} \quad (8)$$

where $\mathit{ID\_allowable}(s)$ = ID's for the s'th pair of allowed attempts. Note due to the interdependence constraint in Eq. (5), it is not allowed for any attempt to be part of more than one pair of allowed stereo requests. Therefore, if that happens, an attempt must be replicated, and the corresponding multiple allowed pairs relative to that attempt split into each replication, see Figure 4. Note this is computed in the pre-processing. If Eq. (7) equals 0, no attempts of that set of stereo

acquisition are made, and if it equals 2, the complete set s is acquired [39].

4) The acquisition of a request takes up both storage of the satellite memory and energy for maneuvering from the battery. A simplified scenario is considered where both down-link (increased memory) and sun exposure (recharging battery) are neglected, and the available levels are thereby known prior. For a longer scheduling horizon, this should be modified. We consider the following:

$$\sum_{i \in N} M_{i,t} x_i \leq m_t \quad \forall t \in \Omega \tag{9}$$

$$\sum_{i \in N} E_{i,t} x_i \leq e_t \quad \forall t \in \Omega \tag{10}$$

where $M_{i,t}$ represents the memory usage of attempt i of satellite t. Note Ω represents the set of satellites, and m_t represents the upper threshold of memory capacity for that particular time horizon. $E_{i,t}$ represents the approximated energy consumption for the maneuver of attempt i for satellite t, while e_t represents the available energy for satellite t in the planning horizon.

5) Lastly, the decision variable is of binary characteristic:

$$x_i \in \{0, 1\} \quad \forall i \in N \tag{11}$$

Note from the perspective of model formulation, Perea et al. [40] ignored the impact of stereo imaging, memory, and energy (Eq. (7)-(10)); Wang et al. [41] ignored stereo, strip, energy, and memory (Eq. (5)-(10)); Bensana et al. [42], Jang et al. [8], Xu et al. [43], and Valicka et al. [44] ignored stereo constraints. Additionally, the way we introduced maneuvering feasibility (Eq. (3)-(4)) to consider the reachable request in near real-time and stereo images (Constraints (7-8)) is also quite new, and it reduces the computational complexity.

D. EXTENDED LONGEST PATH ALGORITHM

The ELPA has been developed to take advantage of the inherent structure of the network of attempts in the SIASP. It requires no parameter tuning, has lower computational effort, and can easily accommodate the multi-satellite framework and the stereo and strip imaging characteristics of the requests. Utilizing a heuristic that uses the graph representation is not novel; however, designing one that implements the strip, stereo, and multi-satellite framework is. The ELPA modifies the classical Longest Path Algorithm (LPA).

For a regular DAG, it is possible to identify the longest path by utilizing a topological sorting of the nodes in G and after that employ the LPA [45]. The computational complexity of the LPA is $\mathcal{O}(E + N)$, where E and N are the number of edges and nodes, respectively. The LPA linearly determines the longest path for each node from one end to another. This is possible as the topological sorting sorts the nodes in relation to how they appear in the DAG. However, as interdependencies exist in the DAG-IAN, this is

Algorithm 1 Extended Longest Path Algorithm for a Weighted DAG-IAN With Interdependent Nodes

Result: Longest weighted path in the directed acyclic graph with interdependent and allowed nodes G

G:= matrix representation of the topologically sorted DAG-IAN representing edges between nodes i and j
B:= matrix representation of interdependencies between nodes i and j
b:= vector representation of the max number of acquisitions for each interdependent node i
A:= matrix representation of all pairs s of allowed stereo attempts i
w:= vector representation of the weight for each node
α:= depth variable
Longest_path:= list w/ longest path for each node
path_weight:= list w/ weight of longest path for each node
for *each node i in G* **do**
    //identify longest allowable path to i
    Incomming_paths:= subset of Longest_paths leading into node i, sorted by path_weight and with no more elements than α
    if *Incoming_neighbours* = $\emptyset$ **then**
        x:= binary representation of the path with only node i
        if $Ax = \{0, 2\}$ **then**
            Longest_path[i]:= x
            path_weight[i]:= wx
        else
            Longest_path[i]:= []
            path_weight[i]:= 0
        end
    else
        for *each incoming path* $j \in$ *Incoming_neighbours* **do**
            x:= binary representation of the path j with node i
            Longest_path_temp:= temporary list w/ longest path for each path
            path_weight_temp:= temporary list w/ weight of each path
            if $Bx \leq b$ **then**
                if $Ax \in \{0, 2\}$ **then**
                    if $j = 1$ **then**
                        Longest_path[i]:= x
                        path_weight[i]:= wx
                        break
                    else
                        Longest_path_temp[j]:= x
                        path_weight_temp[j]:= wx
                    end
                else
                    //add stereo attempts
                    stereo_i:= node prior to i that completes stereo request
                    if *stereo_i* = $\emptyset$ **then**
                        Longest_path_temp[j]:= []
                        *path_weight_*[j]:= 0
                    else
                        x_stereo:= INSERT(x, *stereo_i*)
                        Longest_path_temp[j]:= *x_stereo*
                        path_weight_temp[j]:= w *x_stereo*
                        break
                    end
                end
            else
                //remove the least contributing interdependent node
                if *node i is not a stereo request* **then**
                    interdep_i:= interdependent nodes in path x relative to node i
                    min_illegal_node:= smallest weighted node in interdep_i
                    Longest_path_temp[j]:= REMOVE(x, *min_illegal_node*)
                else
                    illegal_stereo_node:= nodes in A that complete the same stereo request as node i
                    stereo_inter_n = nodes in A that together with i complete stereo constraint
                    x:= REMOVE(x, *illegal_stereo_node*)
                    illegal_stereo_node:= INSERT(x, *stereo_inter_n*)
                end
            end
        end
        Longest_path[i]:= highest weighted path in *Longest_path_temp*
        path_weight[i]:= weight of *Longest_path*[i]
    end
end
RETURN(highest weighted path in *Longest_path*)

TABLE 1. Notation table for problem formulation.

Indices	
N	Number of imaging attempts ($i \in \{1, \ldots, N\}$)
R	Number of unique requests ($r \in \{1, \ldots, R\}$)
S	Number of complete pairs of stereo requests ($s \in \{1, \ldots, S\}$)
Parameters and Matrices	
c_i	the relative value of image attempt i with respect to all the other attempts and criteria
$G_{i,j}$	Binary matrix that represents all feasible maneuvers between any two attempts $\{i, j\}$
$B_{r,i}$	Binary matrix that for any unique request r yields which attempts that represent particular request
b_r	Maximum number of acquisition per request r
$A_{s,i}$	Matrix yielding which pairs of attempts that can be acquired in order to complete a stereo request, i.e. a request of two attempts acquiring the same area where the convergence angle between these two attempts are between 15^o-20^o. (Value of 1 indicating first acquisition in the pair s, and 0 indicating attempt that are not part of the sth pair)
$E_{i,t}$	The energy consumption for satellite t on attempt i
e_t	Maximum energy capacity for satellite t
$M_{i,t}$	The memory consumption for satellite t on attempt i
m_t	Maximum memory capacity for satellite t
Decision variables	
x_i	Binary variable that represents either an included or excluded ith acquisition

Algorithm 2 Pseudocode Representing How to Remove a Non-Allowable Node I in a Path p as REMOVE(p,I)

Result: remove node I in path p
p:= list with all nodes in path
I:= node in G which should be removed from p
x:= binary vector representation of path p
$x_I := 0$
//search for alternative nodes
a:= the last node before I included in the path p
b:= the first node after I included in the path p
r:= range of interest, i.e., list of nodes between node a and b
F_n:= nodes in the range r that connect nodes a and b relative to G
if *F_n is empty* **then**
  RETURN(x)
else
  Longest_path_temp:= temporary list w/ longest path for each alternative
  path_weight_temp:= temporary list w/ weight of each alternative
  for *each node k in F_n* **do**
    x_temp:= binary representation of the modified path p' with feasible node k and without the removed node I
    if $Bx\_temp \leq b \wedge Ax\_temp = \{0,2\}$ **then**
      $Longest\_path\_temp_k := x$
      $path\_weight\_temp_k := wx$
    end
  end
  RETURN(highest weighted path in *Longest_path_temp*)
end

Algorithm 3 Pseudocode Representing How to Add a Node I to the Path p as INSERT(p,I)

Result: insert node I in path p
p:= list with all nodes in path p
I:= node in G which should be added to path p
x:= binary vector representation of path p
$x_I := 1$
//check for violations
if $Bx > b$ **then**
  //violating number of interdependent nodes
  interdependent_n:= nodes in p that are interdependent with node I
  remove_i:= node with smallest weight in *interdependent_n*
  x:= REMOVE(x, remove_i)
end
if $Ax \neq \{0,2\}$ **then**
  //violating stereo constraint
  stereo_inter_n = nodes in p that together with I violate stereo constraint
  remove_i = node with smallest weight in stereo_inter_n
  x:= REMOVE(x, remove_i)
end
if $\exists i \in N : x_i + x_I = 2 \wedge (G[i, I] = 1 \vee G[I, i] = 1)$ **then**
  //violating maneuverability
  remove_i = i, which violates the above if-statement
  x:= REMOVE(x, *remove_i*)
end
RETURN(x)

not sufficient, and the regular longest path algorithm must be extended to satisfy the additional constraints. A pseudocode of the proposed extension can be seen in Algorithm 1.

There are three fundamental phases, which the ELPA iteratively goes through for each node: a ranking phase of the incoming paths to the current node based on the path lengths; a correction phase where paths are investigated and corrected based on the constraint it is violating; and lastly, a searching phase where another node is sought to be included as an alternative to the correction made in the previous phase. The traditional LPA only consists of the ranking phase, and consequently, the ELPA is a two-loop version of the LPA in which the correction phase and the path are investigated, and depending on its state relative to the interdependency and stereo constraints, a fitting correction procedure can be determined.

For the ELPA, only one of the following four scenarios is true for a step-wise generated path when adding node i:

1) $Bx \leq b \wedge Ax \in \{0, 2\} \Rightarrow$ The path is acceptable as it is not violating any constraints. The search phase is, therefore, omitted.
2) $Bx \leq b \wedge Ax \notin \{0, 2\} \Rightarrow$ The path is missing a stereo attempt to yield a complete stereo request.
3) $Bx > b \wedge Ax \in \{0, 2\} \Rightarrow$ The path incorporates too many interdependent nodes, and the smallest weighted interdependent node relative to node i should be removed.
4) $Bx > b \wedge Ax \notin \{0, 2\} \Rightarrow$ The path is incorporating another complete pair of stereo attempts, so to fix this, the pair should be removed, and another stereo attempt should be included to yield a complete stereo request.

When modifying a path by removing a non-stereo node, two things must be true: the path will still satisfy the stereo constraint, and it is possible that another alternative node

could replace the removed one. The ELPA is designed only to remove a complete pair of stereo attempts (a complete stereo request) to include another stereo attempt of the same request. For that modification, the procedure is the same, where another node is searched for as an alternative to that node. Ideally, an entire alternative set of nodes could replace the removed nodes, but the algorithm omits this as the search for a set is very computationally expensive.

When inserting a node that does not follow the order of the DAG-IAN, the maneuverability constraint is not necessarily preserved. Therefore, one has to check for both interdependency and stereo constraint. If any constraints are violated when inserting a node, the responsible nodes in the path (not the inserted and the last node) are removed, and an alternative node to the removed node will be searched for. As the algorithm only goes through two loops when traversing the DAG-IAN, the optimal path can sometimes be neglected. This is because the algorithm, in searching for an alternative node to a removed one, is not allowed to also search in the set of alternative nodes that violate a constraint. Doing so would have made the ELPA a three-loop version of the LPA. If the optimal solution should be ensured, then by continuing the extension, that version of the ELPA would have a worst-case complexity of $\mathcal{O}(N^N)$.

Moreover, for operational purposes, we have included a depth variable, which determines the maximum number of incoming paths that are investigated and modified for each node. The increasing performance and time complexity are illustrated for different depth variables in Table S3 of the Supplementary file. Based on that table, we set the depth variable to 25. Note the computation of each path is independent of the others, so it is possible to compute this in a parallel manner, thereby overruling the need for the depth variable. For reasons of comparison, this is not done in our research.

The worst-case computational complexity of the ELPA is $O(mN^3)$; see the calculation in Section S-IV of the Supplementary file. The average-case complexity is, however, expected to be much better, as the investigated set of nodes in the ELPA when utilizing the remove and insert operator is between the prior and later node and not the entire set of nodes. Consequently, We can assess the ELPA to have a worst-case computational complexity of the ELPA is $O(mNR^2)$, where R is the maximum number of attempts between any two scheduled attempts. The worst-case complexity of the ELPA makes it comparable to that of the dynamic programming algorithm presented in the works of Lemaitre et al. [2], which have a time complexity of $O(|B|^2 \times max_i T_i)$, where B is the number of imaging attempts in the problem scenario and $max_i T_i$ is proportional to the inverse of the time discretization interval.

For a thoroughly explained example of the ELPA used on the problem of Figure 5, see Supplementary file S-3. As an a posteriori check, the solution approach should integrate a search for the longest path that does not violate the memory and energy constraint in Eq. (6).

E. GREEDY AND RANDOM SOLUTION ALGORITHMS

For comparison, we use two solution algorithms often applied in the literature. One is a greedy approach, which iteratively adds the highest-scored node to the solution and checks whether the objective function is improved. If improved, the node is added. The random approach performs the selection based on a random distribution. To direct the exploration phase of the approach, the probability distribution is weighted based on the corresponding score of the nodes relative to the total score of all nodes.

Due to the constraints and interdependencies on the solution space, adding a single node will likely make the solution infeasible. Therefore, the addition of a node is done based on the principles of the INSERT operator showcased in Algorithm 3.

F. ALGORITHM PERFORMANCE

The performance of the ELPA and DAG-IAN formulation is compared with the GNU Linear Programming Kit (GLPK) implemented in the CVXOPT package, which is widely used for large-scale mixed-integer linear programming problems [46]. As version 1.3.0 of the GLPK implementation offers an exact solution approach, the performance in objective value is expected to be higher than that of the ELPA [47]. All simulations are run on a workstation with a 1.6 GHz Intel i5-8250 processing unit.

As seen in Table 2, the deviation in objective value performance between the exact approach and the ELPA is maximum 2% [15], [48]. The Random and Greedy approaches are much more sporadic in performance, as for large scenarios when the exact approach cannot deliver a solution, they can be as far as 70 % away from the objective function value of the ELPA. For small problem scenarios, the exact approach is the most efficient option. Still, as it almost randomly stops being able to obtain a solution, it is not useful for larger problem scenarios. The problem is complexity depends on the number of nodes $|N|$ but especially the number of interdependent sets $|B|$. When $|B|$ is high, the performance of the ELPA is much higher than that of the greedy and random approaches.

G. OUTCOME OBJECTIVES

Despite the intuitiveness behind the scoring procedure, it becomes challenging to ensure the preferences due to problem complexity and scale, as well as variations in problem scenarios, cross-agendas, and incompetence in the operation. Consequently, it is challenging for the satellite operation to agree on a common preference setting. This is especially the case, as the input is the weight setting of the ELECTRE-III, which allow for a high degree of customizability. Effectively, the outcome objectives provide the DMs with the ability to integrate a posteriori tuning of the a priori preference structure.

In other research, the objective function representing the preferences of the DM is generic or very simple, and

TABLE 2. Comparison of the computational complexity and relative performance of the scheduling methods. The scenario size is denoted by $|N|$, $|E|$, $|B|$, and $|A|$ representing the number of nodes (attempts), number of edges (feasible maneuvers), number of interdependent set of nodes (requests), and number of allowed nodes (set of stereo pairs), respectively. The input for the scenario generator is for reproducibility.

Problem scenario				Performance of scheduling method										Scenario generator	
characteristics				Runtime				Gap to optimal solution (GLPK) and Performance						input	
nodes	edges	int sets	allow sets	GLPK	ELPA	greedy	random	ELPA		Greedy		Random		τ	requests
$\|N\|$	$\|E\|$	$\|B\|$	$\|A\|$	(sec)	(sec)	(sec)	(sec)	gap (%)	(F)	gap (%)	(F)	gap (%)	(F)	(sec)	No.
384	72,739	82	0	0.001	1.130	0.385	0.285	1.2	(69.226)	14.2	(60.068)	11.1	(62.283)	21	500
445	97,648	82	7	0.016	1.715	0.607	0.570	1.4	(70.266)	21.7	(55.744)	26.5	(52.328)	18	500
523	135,280	11	0	0.001	5.911	0.348	0.395	0.0	(8.989)	7.8	(8.292)	3.2	(8.699)	2	65
551	149,766	82	30	0.023	3.526	1.402	1.336	1.3	(72.049)	7.8	(60.036)	34.6	(47.754)	15	500
664	217,491	82	11	0.212	4.273	1.401	1.000	0.9	(74.095)	17.6	(61.635)	2.9	(65.122)	12	500
759	282,708	9	181	0.006	20.778	7.805	9.883	0.0	(8.568)	11.4	(7.594)	5.5	(8.097)	2	50
911	409,571	83	49	-	9.155	3.689	3.571	-	(75.382)	-	(62.504)	-	(50.192)	10	500
949	437,725	14	179	0.001	63.047	15.850	17.131	0.0	(14.086)	13.5	(12.186)	2.3	(13.760)	2	80
1,264	784,862	23	110	0.035	76.988	11.666	15.040	0.2	(18.712)	7.0	(17.430)	6.0	(17.623)	2	146
1,364	907,730	17	344	0.055	555.708	152.720	136.752	0.0	(13.851)	18.8	(11.252)	7.4	(12.834)	2	110
1,407	977,110	83	95	-	22.457	9.610	9.786	-	(76.618)	-	(62.418)	-	(50.669)	6	500
1,753	1,517,822	178	121	-	23.739	22.014	10.154	-	(133.496)	-	(48.394)	-	(77.298)	10	1,000
1,782	1,558,594	17	595	0.392	234.031	157.556	116.375	0.0	(16.581)	33.4	(11.050)	8.2	(15.222)	2	95
1,846	1,683,176	189	123	-	25.507	19.548	13.365	-	(145.674)	-	(56.272)	-	(82.152)	10	1,050
1,927	1,832,659	198	115	-	27.728	28.887	12.668	-	(156.287)	-	(54.509)	-	(86.195)	10	1,100
2,112	2,182,319	26	532	3.098	235.858	82.312	93.615	0.6	(24.346)	21.8	(19.142)	15.6	(20.661)	2	162
2,288	2,586,951	135	180	-	51.302	32.032	16.210	-	(114.891)	-	(48.105)	-	(68.175)	6	750
2,332	2,667,270	32	470	-	961.296	130.585	102.521	-	(26.638)	-	(24.398)	-	(24.982)	2	194
2,342	2,710,406	140	143	-	50.211	46.889	13.725	-	(108.986)	-	(34.979)	-	(62.463)	6	775
2,344	2,714,482	143	85	-	46.982	20.339	15.223	-	(109.627)	-	(89.181)	-	(63.859)	6	800
2,608	3,357,531	157	153	-	62.769	53.537	19.119	-	(122.023)	-	(91.696)	-	(63.936)	6	850
2,616	3,377,718	151	279	-	96.818	122.890	55.006	-	(121.592)	-	(46.455)	-	(72.018)	6	825
2,776	3,805,469	161	284	-	120.063	141.759	51.331	-	(122.840)	-	(75.943)	-	(68.890)	6	875
2,806	3,890,527	166	224	-	100.367	63.203	39.792	-	(130.481)	-	(58.501)	-	(76.311)	6	900
2,826	3,945,712	170	193	-	84.002	46.332	36.192	-	(132.162)	-	(87.482)	-	(73.072)	6	925
2,838	3,978,792	173	157	-	76.458	188.372	35.062	-	(137.222)	-	(44.919)	-	(72.116)	6	950
2,943	4,280,259	174	271	-	124.098	146.304	65.779	-	(133.806)	-	(46.880)	-	(77.439)	6	975
3,260	5,252,687	83	416	-	223.225	195.485	88.103	-	(78.534)	-	(66.703)	-	(54.659)	2	500

due to the complexity of both the scoring and scheduling procedure, as well as the uncertainty in the information, the resulting schedule can very well exhibit preferences that are different from what the DM intended [49]. Therefore, we construct outcome objectives that reflect the resulting schedule both in terms of behavior and performance but are defined directly on the outcome of the schedule. This yields a much more precise evaluation, allowing the DM to have a quantifiable compromise when determining a common preference structure. We choose the following simple outcome objectives for performance:

1) Minimize average observed cloud cover
2) Maximize the total number of acquisition

Furthermore, we define these simple behavioral outcome objectives:

3) Are any priority 2, 3, or 4 requests chosen instead of a priority 1 request?
4) Are any requests with an age less than 13 days chosen instead of a 13 or more days old request?

Based on these objectives, the DM effectively seeks a compromise solution where trade-offs can be quantified rather than imposed by hard constraints. Note that the performance objectives are numerical, and the range depends on the measure of interest. In contrast, the behavioral objectives are binary, with 1 representing an acceptable behavior in the schedule and 0 representing an unacceptable behavior. These outcome objectives are all conflicting, e.g., the lowest average observed cloud cover (in the extreme case) is obtained through the weight setting that leads to only a single acquisition with the smallest cloud cover to be scheduled, which contradicts acquiring the highest possible number of requests. The extensive simulation evaluated with these objectives provides the DMs with the expected outcome of their decisions prior to making them.

H. WEIGHT SPACE ANALYSIS (WSA)

The WSA serves a dual purpose in a decision support context. First, it includes a simulation study that explores the impact of different intervals on the feasible weight space. Second, it incorporates a significance test to identify significant changes to the current preference structure. This means the WSA provides the DM with increased understanding of the decision environment as well as provide suggestions to which modifications one ought to make.

The inspiration for the WSA springs from the research field of Stochastic Multi-criteria Acceptability Analysis (SMAA), which is often applied when criteria and preference information are uncertain, inaccurate, or partially missing [50]. It can also be utilized to understand trade-offs, align groups of DMs, or analyze the robustness perspective of the preference model parameters by exploring the weight space through some assumed utility function and stochastic criteria values.

In MCDM literature, the weight space refers to the range of variable combinations DMs can use to express their prefer-

TABLE 3. Table representing the WSOI. It holds the range limits for the different threshold values investigated in the WSA. Note the DM correspondingly does not assert a specific preference structure but a range within where their intended preference structure could be.

Criteria	lower	upper
area (km2)	0	10000
angle (degrees)	0	45
sun elevation (degrees)	0	90
cloud cover (%)	0	100
priority	0	4
Customer type	0	2
Price (euro)	0	20000
age (days)	0	14
uncertainty (σ^2)	0	2

ences. Our approach extends this by including the threshold values, which also affect the scoring procedure, making a specific combination of weights and threshold values equivalent to the DM's preference structure. The weight space of interest (WSOI) defined by the DM for the threshold values is shown in Table 3, i.e., the range reflected by the lower and upper bound for each threshold variable. Note the WSOI for the weights of each variable is non-trivial as an experienced DM with pre-existing knowledge of their preferences is expected to have a more refined (smaller) WSOI.

The interesting aspect of this WSA is to explore how the outcome objectives behave in the different regions of the weight space and whether some regions are more favorable for all objectives. To investigate this, we choose to separate the ranges of the weights and each criteria range observed in Table 3 into 10 uniform regions. However, due to dependencies and the high dimensionality, that corresponds to $10^{4\times9}$ different combinations of regions, which is infeasible to analyze. Note for the 10 regions to investigate, there are four parameters for each of the nine criteria in the ELECTRE-III model. However, for a large number of simulations, it is expected that some regions of the weight space will produce significantly different outcome objectives compared to other regions of the same criteria. The average outcome objective for a region l is utilized as a metric to compare different regions.

$$\mu_{obj_{1_l}} = \frac{\sum_{h\in H_l} obj_{1_{n_l}}}{|H_l|}, \tag{12}$$

where H_l is the set of instances that fall within region l, each of the hth observed values of objective-1 in region l is denoted $obj_{1_{h_l}}$, and $|H_l|$ represents the total number of instances in region l. Here, suppose we want to obtain an accuracy κ with a 95% confidence interval. In this case, we can consider the observations of the simulation to be point estimators for the outcome objectives of each interval, as well as assuming the average outcome objectives to be normally distributed for each interval given the central limit theorem. Accordingly, the number of simulations required for stated accuracy in each interval is $\frac{Z_\alpha^2}{4\kappa^2}$ [51], [52]. For an accuracy κ of 0.025, the number of simulations required for each region is $\frac{1.96^2}{4*0.025^2} = 1537$.

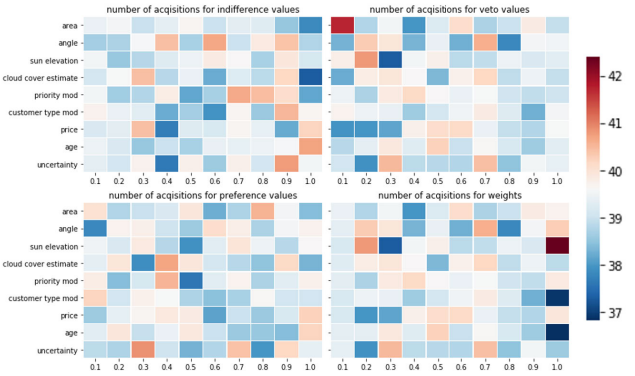

FIGURE 6. Heat plot representing the average number of acquisitions obtained from different ranges seen through 20,000 simulations.

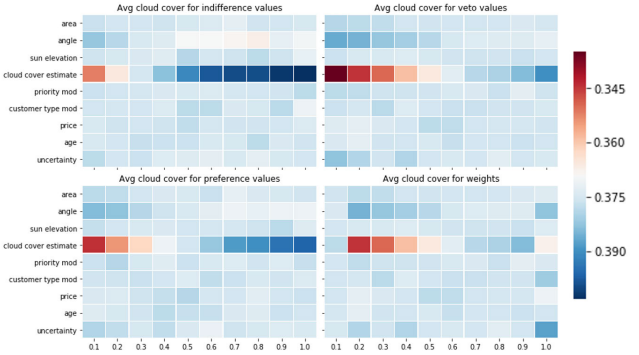

FIGURE 7. Heat plot representing the average cloud cover obtained from 20,000 simulations.

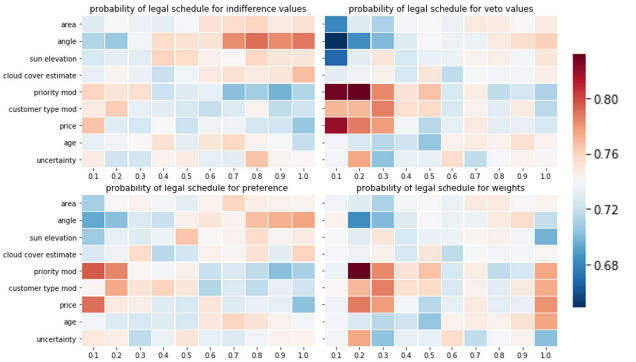

FIGURE 8. Heat plot representing the frequency of following the priority outcome objective obtained from 20,000 simulations.

For this reason, we conduct 20,000 simulations, where the scenarios are generated based on 2,000 worldwide-located customer requests and a two-second temporal resolution on the satellite path, as well as the information previously mentioned in Section III-A. The results from the WSA are empirical and allow the DM to include their experience on the range and, thereby, the significance of the difference between measures.

To identify improving modifications on the preference structure, we compute a significance test that utilizes the computed experiments and a linear model for both the continuous and binary response variables. We then define the predictive variables as categorical variables where the specific segment that each parameter belongs to yields the

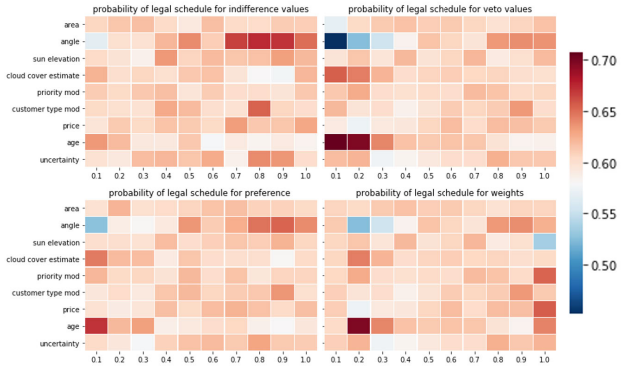

FIGURE 9. Heat plot representing the frequency of following the delivery time or age outcome objective obtained from 20,000 simulations.

value. This is due to the knowledge that each parameter does not necessarily have a linear effect on the objectives. We report the p-values to represent the significance of each interval, that is, the null hypothesis that the group means are not different from the others. By utilizing categorical variables, the test represents how significant the change from an assumed base model to another model is. That is, a specific interval is chosen instead of the one occurring in the base model. Note the base model refers to the assumed preference structure. Accordingly, the first segment will be incorporated into the intercept, and the effect of moving from one segment to another can be evaluated. Additionally, the categorical features ensure that two segments of the same parameter cannot be incorporated at the same time. Before the simulation is conducted, a base preference structure must be defined by the DM as the intercept. We assume, for simplicity, the base preference structure to be the first segment of each parameter in the WSOI.

$$Y_i = \beta_0 + \sum_{j=1}^{N} \beta_j Q_{i,j} + \sum_{l=1}^{N} \beta_l P_{i,l} + \sum_{m=1}^{N} \beta_m V_{i,m} + \sum_{n=1}^{N} \beta_n W_{i,n}$$

$$R_i = \gamma_0 + \sum_{j=1}^{N} \gamma_j Q_{i,j} + \sum_{l=1}^{N} \gamma_l P_{i,l} + \sum_{m=1}^{N} \gamma_m V_{i,m} + \sum_{n=1}^{N} \gamma_n W_{i,n} \forall i \in I$$

where Y_i is the continuous response variable, R_i is the binary response variable, β and γ are the linear regression parameters for the continuous and binary response variable, respectively, and Q_i, P_i, V_i, and W_i are the categorical variables of each segment i on the WSOI.

IV. RESULTS AND DISCUSSION

The results of the simulation are presented via the heatmaps in Figures 6, 7, 8, and 9 and the p-values of Table 5, 4, 6, and 7 indicate the significance of modifying the assumed base model.

The decision process of the operator can be seen in In Figure 10, where the input (WSOI, number of intervals, outcome objectives, and base preference profile) to output (outcome objectives) relations can be investigated in greater detail through the WSA. Additionally, the operator also is suggested significant updates based on the significance test results.

Consequently, the operator can through the WSA in Figure 7 obtain the recommendation for minimizing the average observed cloud cover as the following: set an indifference value less than 0.2 of the range previously stated in Table 3, i.e., a value of 20%; preference value of less than 30%; veto threshold of less than 40%; and surprisingly, a weight between 0.1 and 0.5 or of more than 0.9. The preferred ranges of weight are probably due to the fact that a higher weight will exclude the information stated in the threshold values. This means the uncertainty information will be completely excluded. Interestingly, this result mimics some of the characteristics presented by Braess' paradox [53]. Furthermore, the angle parameters should be set at a higher indifference, preference, and veto threshold, where the indifference threshold, in particular, should be set in between 0.4 and 0.8 of the defined criteria limit. In general, this means that one should neglect the influence of incidence angle when minimizing cloud cover. Similarly, if one were to make changes compared to the assumed base preference structure, then for the cloud objective, any change in the cloud coverage parameters would lead to a significant change, as well as the latter segments of any of the uncertainty and depointing angle parameter segments. See Figures. 5-7.

For maximizing the number of acquisitions, we can deduce the following recommendations based on Figure 6: generally set a high indifference threshold for all criteria (especially angle and uncertainty); generally set a high preference threshold and veto threshold; and refrain from setting high weights for any single criterion and therefore small weights for the others. This means to set as equal weights as possible. For this outcome objective, the large multi-dimensionality becomes a problem, and a smaller WSOI should be analyzed to uncover it better.

To follow the behavioral objective of always acquiring priority 1 over priority 2,3, and 4, it can be seen in Figure 8 that the DM should set a higher indifference value for angle, cloud cover, and age while setting low indifference thresholds for priority, type, and price; the same pattern applies to the preference threshold; set high veto thresholds for all criteria except priority, type, and price; set weights s.t. priority, type, and price in the range of $0.1 - 0.4$ of its limit, while the others should be in the first part of the range. Note that a higher priority weight does not necessarily lead to acceptable behavior; e.g., the weight for priority, type, price, and age should be either the lower or higher segments of the range.

To follow the behavioral objective of always acquiring requests with an age of 13 days or more relative to requests with a lower age, it can be recommended that indifference thresholds, in general, should be high for all criteria except

TABLE 4. The p-values of the different segments of the indifference threshold parameters computed for the four objectives; maximizing the number of acquisitions (UL), minimizing average cloud coverage (UR), accommodating the behavioral priority outcome (LL), and accommodating the behavioral age outcome (LR), respectively.

	[.1,.2)	[.2,.3)	[.3,.4)	[.4,.5)	[.5,.6)	[.6,.7)	[.7,.8)	[.8,.9)	[.9,1]	[.1,.2)	[.2,.3)	[.3,.4)	[.4,.5)	[.5,.6)	[.6,.7)	[.7,.8)	[.8,.9)	[.9,1]
area	0.50	0.73	0.92	0.73	0.83	0.65	0.44	0.44	0.43	0.65	0.72	0.17	0.68	0.91	0.35	0.24	0.54	0.85
angle	0.64	0.34	**0.04**	0.98	0.11	0.58	0.31	0.21	0.84	0.31	**0.00**	**0.00**	**0.00**	**0.00**	**0.00**	**0.00**	**0.00**	**0.00**
sun	0.23	0.52	0.93	0.92	0.87	0.94	0.46	0.83	0.54	0.42	0.52	0.28	0.18	0.80	0.58	0.19	0.38	0.58
cloud	0.26	**0.05**	0.85	0.51	0.74	0.67	0.93	0.37	0.53	**0.00**	**0.00**	**0.00**	**0.00**	**0.00**	**0.00**	**0.00**	**0.00**	**0.00**
priority	0.23	0.27	0.88	0.26	0.36	0.32	0.41	0.94	0.11	0.67	0.62	0.71	0.59	0.97	0.75	0.43	0.33	0.29
type	1.00	0.86	0.24	0.50	0.25	0.92	0.47	0.23	0.43	0.66	0.93	0.60	0.09	0.37	0.86	0.89	0.31	0.13
price	0.68	0.41	**0.03**	0.75	0.92	0.83	0.77	0.10	0.64	0.69	0.56	0.95	0.20	0.80	0.16	0.61	0.93	0.36
age	0.80	0.44	0.83	0.90	0.55	0.40	0.30	0.43	0.32	0.81	0.41	0.48	0.47	0.65	0.41	**0.05**	0.87	0.41
uncertainty	0.35	0.88	**0.05**	0.81	0.22	0.99	0.74	0.51	0.96	0.45	0.84	0.09	0.15	**0.04**	0.16	0.10	0.49	0.40
area	0.77	0.78	0.51	0.93	0.42	0.33	0.13	0.26	0.21	0.59	0.39	0.74	0.21	0.83	0.77	0.62	0.71	0.78
angle	**0.05**	0.81	0.14	0.34	0.56	**0.02**	**0.01**	0.08	0.06	0.73	0.93	0.41	0.10	0.82	**0.01**	**0.00**	**0.00**	**0.03**
sun	0.45	0.40	0.27	0.27	0.67	0.91	0.25	0.44	0.32	0.52	0.18	0.07	0.67	0.43	0.43	0.34	0.08	0.10
cloud	0.94	0.78	0.21	0.87	0.59	0.39	0.67	0.62	0.47	0.52	0.62	0.66	0.17	0.09	0.55	0.78	0.69	0.16
priority	**0.02**	**0.00**	0.25	0.06	**0.04**	0.78	0.26	0.58	0.24	0.79	0.38	0.35	0.50	0.63	0.86	0.93	0.56	0.82
type	0.26	0.34	0.68	0.95	0.98	0.87	0.36	0.65	0.97	0.28	0.21	0.51	0.79	0.42	0.40	0.10	0.65	0.99
price	0.08	0.16	0.80	0.20	0.95	0.98	0.65	0.97	0.91	0.15	0.54	0.24	0.39	0.70	0.06	0.23	0.26	0.11
age	0.38	0.29	0.18	0.65	0.81	0.56	0.91	0.90	0.25	0.45	0.48	0.96	0.45	0.14	0.55	0.43	0.63	0.27
uncertainty	0.08	0.14	1.00	0.65	0.79	0.73	0.20	0.94	0.61	0.83	0.11	0.21	0.47	0.18	0.31	0.10	**0.05**	0.73

age, and the same applies for the preference and veto threshold. The weight of all other criteria does not affect the behavioral objective. However, the preferred range for the weight of age should be $0.1 - 0.3$. Due to the timely delivery requirement, the DM may need to sacrifice the quality criteria; this is also reflected in Figure 9 where angle, sun elevation, and even customer type are closely related to upholding this objective.

It is clear that these outcome objectives are conflicting; however, when describing the preference structure through this weight space, it is easier to find trade-offs between the objectives, as one can quantify and evaluate them based on informed grounds. For example, for the outcome objectives of cloud cover, priority, and age, one can observe the general proposal of setting a high indifference, preference, and veto threshold for the area, angle, and sun elevation criteria. Another common trait for these three objectives is to set low indifference, preference, and veto threshold values for the priority, type, and price criteria.

Most studies fail to consider the multi-criteria nature of the problem, and they, therefore, ignore the aggregated impact of some specifications in the scheduling. From our analysis, we can observe that the indifference, veto threshold values, and weights provide the DM with much more flexibility and allow for the integration of a more robust preference structure. In general, adding information about the uncertainty of preferences through fuzzy sets can leverage the decision-making environment significantly [54].

A. MANAGERIAL IMPLICATIONS

In a typical operational context, to make the best use of satellite resources, the DM needs to express their preferences accurately in order for the outcome of the scheduling process to meet their expectations. To that extent, priorities are assigned to each request, and scores are computed for each imaging attempt depending on the criteria given in Table 3. Previous scoring functions, as devised by the satellite operation, are most often an average and weak compromise between the quantity, quality, and timeliness of images delivered by the system. After the scheduling procedure, DMs verify the selection of images by investigating the expected quality of the included and the omitted customer request pool, and if the scheduling output does not meet their expectations regarding customer requirements, their options are limited to changing request priorities, or suspending / re-submitting requests to influence the subsequent cycles of the scheduling procedure. The decision process of the proposed approach is illustrated in Figure 10 and provides the following benefits to improve satellite operations:

- The MCDM framework (here based on ELECTRE-III) provides more insight into the different criteria through indifference, preference, and veto thresholds, while the weight can be set differently depending on the type of request, customer, or application. Additionally, it provides the capability of an intuitive a priori integration of preferences which is compatible with future operational requirements.
- The scheduling algorithm based on the ELPA provides a good compromise between the quality of the schedule and the run-time performance, such that operators can quickly get feedback on how their preferences may translate into a feasible schedule. Additionally, it incorporates the multi-satellite framework, exploiting the information symmetry of a centralized approach. Similarly, it accommodates the stereo and strip request characteristics.
- The WSA can be performed offline on a number of typical scenarios to provide critical insight into how the criteria weights and thresholds actually affect the resulting schedule performance objectives. The significance test allows the DM to identify significantly positive corrections to the preference structure, and the operators can locate a way to fix the threshold for each criterion.

B. PERSPECTIVATION

The multi-criteria decision-making framework, the ELPA, and the decision support information to the DM here

TABLE 5. The p-values of the different segments of the preference threshold parameters computed for the four objectives; maximizing the number of acquisitions (UL), minimizing average cloud coverage (UR), accommodating the behavioral priority outcome (LL), and accommodating the behavioral age outcome (LR), respectively.

	[.1,.2)	[.2,.3)	[.3,.4)	[.4,.5)	[.5,.6)	[.6,.7)	[.7,.8)	[.8,.9)	[.9,1]	[.1,.2)	[.2,.3)	[.3,.4)	[.4,.5)	[.5,.6)	[.6,.7)	[.7,.8)	[.8,.9)	[.9,1]
area	0.64	0.83	0.95	0.63	0.42	0.81	0.21	0.56	0.91	0.71	0.44	0.07	0.13	0.68	**0.03**	0.13	0.24	0.43
angle	**0.03**	**0.01**	0.14	0.25	**0.03**	0.07	0.30	0.22	0.12	0.45	0.76	0.85	0.55	0.98	0.40	0.72	0.94	0.94
sun	0.57	0.21	1.00	0.42	0.83	0.51	0.76	1.00	0.48	0.41	0.11	0.08	0.14	**0.04**	**0.04**	**0.05**	0.40	**0.01**
cloud	0.82	**0.01**	0.90	0.68	0.31	0.26	0.24	0.88	0.32	0.12	**0.05**	**0.00**	**0.02**	**0.00**	**0.00**	**0.00**	**0.00**	**0.00**
priority	0.24	0.68	0.44	0.21	0.69	0.56	0.85	0.82	0.19	0.20	0.75	0.30	0.55	0.91	0.33	0.89	0.30	0.67
type	0.20	0.45	0.46	0.14	0.11	0.18	0.60	0.14	**0.04**	0.77	0.60	0.91	0.36	0.65	0.85	0.48	0.74	0.80
price	0.76	1.00	0.92	0.87	0.26	0.68	0.55	0.88	0.43	0.66	1.00	0.62	0.35	0.55	0.88	0.07	0.70	0.58
age	0.88	0.65	0.90	0.67	0.72	0.42	0.42	0.27	0.98	0.22	0.23	0.13	0.19	0.42	0.92	0.37	0.87	0.94
uncertainty	0.93	0.07	0.61	0.82	0.90	0.19	0.66	0.45	0.84	0.93	0.57	0.74	0.99	0.11	0.21	0.47	0.73	1.00
area	0.22	0.26	0.84	0.99	0.84	0.40	0.91	0.51	0.31	0.88	0.16	0.18	0.59	0.99	0.99	0.62	0.35	0.15
angle	0.77	0.67	0.53	0.66	0.45	0.90	0.41	0.34	0.29	0.37	0.52	0.46	0.35	0.90	0.92	0.92	0.91	0.52
sun	0.77	0.52	0.37	**0.02**	0.51	0.38	0.17	0.77	0.91	0.93	0.66	0.23	0.83	0.57	0.47	0.60	0.67	0.38
cloud	0.42	0.06	0.77	0.72	0.20	0.38	0.17	0.79	0.14	0.32	0.57	**0.03**	0.15	**0.02**	**0.01**	**0.02**	**0.00**	0.06
priority	0.87	**0.02**	**0.03**	0.15	**0.01**	**0.04**	**0.03**	**0.01**	**0.02**	0.22	0.26	0.07	0.58	0.13	0.35	0.10	0.41	0.42
type	**0.01**	0.06	**0.00**	**0.01**	0.57	0.32	0.70	0.08	0.08	0.11	0.14	**0.02**	**0.03**	0.13	0.08	0.15	**0.01**	0.12
price	0.26	0.71	0.38	0.39	0.91	0.17	0.28	0.22	**0.01**	0.25	0.20	0.65	0.26	0.65	0.69	0.32	0.14	0.35
age	0.38	0.18	0.15	0.07	0.51	0.88	0.57	0.32	0.57	0.08	0.94	0.09	0.12	0.62	0.90	0.80	0.74	0.53
uncertainty	0.90	0.33	0.64	0.89	0.26	0.27	0.21	0.34	0.49	0.96	0.40	0.63	0.50	0.62	0.79	0.42	0.84	0.83

TABLE 6. The p-values of the different segments of the veto threshold parameters computed for the four objectives; maximizing the number of acquisitions (UL), minimizing average cloud coverage (UR), accommodating the behavioral priority outcome (LL), and accommodating the behavioral age outcome (LR), respectively.

	[.1,.2)	[.2,.3)	[.3,.4)	[.4,.5)	[.5,.6)	[.6,.7)	[.7,.8)	[.8,.9)	[.9,1]	[.1,.2)	[.2,.3)	[.3,.4)	[.4,.5)	[.5,.6)	[.6,.7)	[.7,.8)	[.8,.9)	[.9,1]
area	**0.05**	0.19	**0.02**	0.07	0.27	**0.05**	**0.05**	0.13	0.07	0.86	0.97	0.93	0.79	0.89	0.96	0.96	0.58	0.73
angle	0.52	0.87	0.14	0.45	0.10	0.70	**0.03**	0.31	0.24	0.20	0.08	**0.04**	**0.01**	**0.00**	**0.00**	**0.00**	**0.00**	**0.00**
sun	0.55	0.07	0.69	0.89	0.62	0.55	0.76	0.70	0.61	0.68	0.90	0.97	0.56	0.30	0.28	0.21	0.22	0.25
cloud	0.29	0.15	0.27	0.81	0.25	0.11	0.34	0.20	0.33	**0.01**	**0.00**	**0.00**	**0.00**	**0.00**	**0.00**	**0.00**	**0.00**	**0.00**
priority	0.92	0.39	0.44	0.57	0.61	0.66	0.92	0.79	0.55	0.56	0.28	0.59	0.45	0.19	0.39	0.62	**0.05**	0.50
type	0.89	0.77	0.95	0.70	0.37	0.18	0.44	0.77	0.18	0.74	0.92	0.28	0.84	0.79	0.76	0.66	0.78	0.40
price	0.91	0.88	0.22	0.15	0.08	0.14	0.21	0.24	0.19	0.51	0.85	0.52	0.13	0.24	0.40	0.38	0.41	0.44
age	0.93	0.53	0.66	0.40	0.99	0.55	0.69	0.88	0.85	0.15	0.63	0.45	0.42	0.66	0.32	0.51	0.82	0.57
uncertainty	0.53	0.50	0.77	0.94	0.97	0.37	0.78	0.74	0.88	0.06	0.06	0.28	**0.01**	**0.05**	**0.03**	**0.00**	0.07	**0.02**
area	0.06	0.49	**0.04**	**0.01**	**0.03**	**0.01**	**0.01**	**0.01**	**0.00**	0.24	0.08	**0.03**	**0.03**	**0.03**	0.07	0.11	**0.03**	**0.00**
angle	0.06	**0.02**	**0.00**	**0.00**	**0.00**	**0.00**	**0.00**	**0.00**	**0.00**	**0.01**	**0.00**	**0.00**	**0.00**	**0.00**	**0.00**	**0.00**	**0.00**	**0.00**
sun	**0.01**	**0.00**	**0.03**	**0.05**	**0.04**	**0.01**	**0.01**	**0.03**	**0.00**	0.58	0.97	0.45	0.71	0.87	0.64	0.28	0.41	0.79
cloud	0.67	0.78	0.38	0.66	0.24	0.76	0.52	0.46	0.45	0.95	0.46	0.17	0.30	0.44	0.44	0.55	0.58	0.54
priority	0.88	**0.04**	**0.00**	**0.01**	**0.00**	**0.00**	**0.00**	**0.00**	**0.00**	0.39	0.83	0.89	0.87	0.78	0.24	0.35	0.49	0.51
type	0.31	0.52	**0.03**	**0.02**	**0.00**	**0.01**	**0.00**	**0.02**	**0.00**	0.17	0.17	**0.02**	**0.04**	0.13	0.09	0.10	0.30	**0.02**
price	0.19	0.16	**0.00**	**0.00**	**0.00**	**0.01**	**0.00**	**0.00**	**0.00**	0.63	0.77	0.81	0.38	0.18	0.66	0.29	0.21	0.36
age	0.70	0.58	0.90	0.47	0.30	0.29	0.45	0.21	0.31	0.74	**0.04**	**0.00**	**0.00**	**0.01**	**0.00**	**0.00**	**0.00**	**0.00**
uncertainty	0.07	0.42	0.58	0.64	0.11	0.92	0.25	0.18	0.26	0.79	0.09	0.16	0.19	0.20	0.25	0.70	0.37	0.45

TABLE 7. The p-values of the different segments of the weight parameters computed for the four objectives; maximizing the number of acquisitions (UL), minimizing average cloud coverage (UR), accommodating the behavioral priority outcome (LL), and accommodating the behavioral age outcome (LR), respectively.

	[.1,.2)	[.2,.3)	[.3,.4)	[.4,.5)	[.5,.6)	[.6,.7)	[.7,.8)	[.8,.9)	[.9,1]	[.1,.2)	[.2,.3)	[.3,.4)	[.4,.5)	[.5,.6)	[.6,.7)	[.7,.8)	[.8,.9)	[.9,1]
area	**0.05**	0.19	**0.02**	0.07	0.27	**0.05**	**0.05**	0.13	0.07	0.86	0.97	0.93	0.79	0.89	0.96	0.96	0.58	0.73
angle	0.52	0.87	0.14	0.45	0.10	0.70	**0.03**	0.31	0.24	0.20	0.08	**0.04**	**0.01**	**0.00**	**0.00**	**0.00**	**0.00**	**0.00**
sun	0.55	0.07	0.69	0.89	0.62	0.55	0.76	0.70	0.61	0.68	0.90	0.97	0.56	0.30	0.28	0.21	0.22	0.25
cloud	0.29	0.15	0.27	0.81	0.25	0.11	0.34	0.20	0.33	**0.01**	**0.00**	**0.00**	**0.00**	**0.00**	**0.00**	**0.00**	**0.00**	**0.00**
priority	0.92	0.39	0.44	0.57	0.61	0.66	0.92	0.79	0.55	0.56	0.28	0.59	0.45	0.19	0.39	0.62	**0.05**	0.50
type	0.89	0.77	0.95	0.70	0.37	0.18	0.44	0.77	0.18	0.74	0.92	0.28	0.84	0.79	0.76	0.66	0.78	0.40
price	0.91	0.88	0.22	0.15	0.08	0.14	0.21	0.24	0.19	0.51	0.85	0.52	0.13	0.24	0.40	0.38	0.41	0.44
age	0.93	0.53	0.66	0.40	0.99	0.55	0.69	0.88	0.85	0.15	0.63	0.45	0.42	0.66	0.32	0.51	0.82	0.57
uncertainty	0.53	0.50	0.77	0.94	0.97	0.37	0.78	0.74	0.88	0.06	0.06	0.28	**0.01**	**0.05**	**0.03**	**0.00**	0.07	**0.02**
area	0.06	0.49	**0.04**	**0.01**	**0.03**	**0.01**	**0.01**	**0.01**	**0.00**	0.24	0.08	**0.03**	**0.03**	**0.03**	0.07	0.11	**0.03**	**0.00**
angle	0.06	**0.02**	**0.00**	**0.00**	**0.00**	**0.00**	**0.00**	**0.00**	**0.00**	**0.01**	**0.00**	**0.00**	**0.00**	**0.00**	**0.00**	**0.00**	**0.00**	**0.00**
sun	**0.01**	**0.00**	**0.03**	**0.05**	**0.04**	**0.01**	**0.01**	**0.03**	**0.00**	0.58	0.97	0.45	0.71	0.87	0.64	0.28	0.41	0.79
cloud	0.67	0.78	0.38	0.66	0.24	0.76	0.52	0.46	0.45	0.95	0.46	0.17	0.30	0.44	0.44	0.55	0.58	0.54
priority	0.88	**0.04**	**0.00**	**0.01**	**0.00**	**0.00**	**0.00**	**0.00**	**0.00**	0.39	0.83	0.89	0.87	0.78	0.24	0.35	0.49	0.51
type	0.31	0.52	**0.03**	**0.02**	**0.00**	**0.01**	**0.00**	**0.02**	**0.00**	0.17	0.17	**0.02**	**0.04**	0.13	0.09	0.10	0.30	**0.02**
price	0.19	0.16	**0.00**	**0.00**	**0.00**	**0.01**	**0.00**	**0.00**	**0.00**	0.63	0.77	0.81	0.38	0.18	0.66	0.29	0.21	0.36
age	0.70	0.58	0.90	0.47	0.30	0.29	0.45	0.21	0.31	0.74	**0.04**	**0.00**	**0.00**	**0.01**	**0.00**	**0.00**	**0.00**	**0.00**
uncertainty	0.07	0.42	0.58	0.64	0.11	0.92	0.25	0.18	0.26	0.79	0.09	0.16	0.19	0.20	0.25	0.70	0.37	0.45

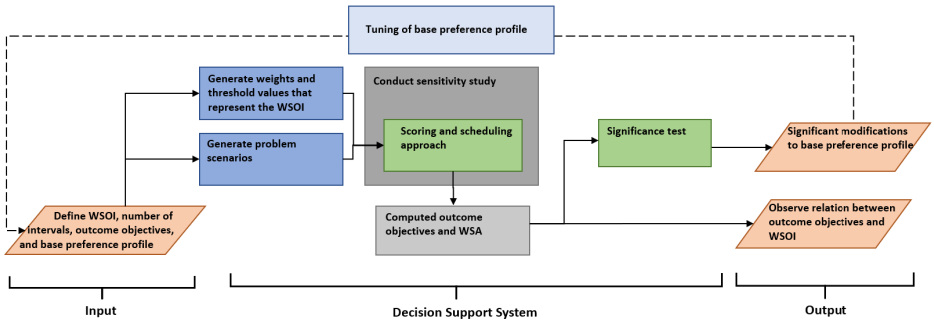

FIGURE 10. A holistic illustration of the decision support system for the DM, indicating how the proposed WSA is developed and how the preference structure can be iteratively improved based on informed suggestions from a significance test. Essentially, aiding the DM in understanding the intricacies of the problem scenarios, the system, and the collaborative effect of the multiple criteria affecting the decision process.

have potential implications beyond the realm of EOS, as they embody principles applicable to various optimization problems - especially when integrating multiple objectives. For instance, in disaster response and relief operations to compromise the many different criteria efficiently and in a scalable manner [55], [56], [57]; healthcare resource allocation for the scheduling of medical staff, equipment, and patient appointments in hospitals to optimize resource use and patient care [58]; fleet management for logistics [59], and urban traffic management to balance the many conflicting requirements [60]. All of these problem domains require the modeling of interdependencies in the solution space, as well as efficient solution approaches that intuitively allow for preference integration out-of-operation for a fast deployment.

V. CONCLUSION

The proposed three-stage solution procedure increases the explainability of the system to human operators. It provides valuable assistance to adequately express preferences and manage conflicting and fluctuating customer requirements in an uncertain environment. Although we consider nine different criteria, the scoring scheme makes the problem context analytically simple, as it is possible to neglect the operational a posteriori integration of preferences or hard constraints associated with the problem. We also found that the ELPA approach seems to perform within 2% of the objective function value compared with an exact solver for smaller problem scenarios, while it efficiently solves large-scale problems, as opposed to the exact approach, which fails. Compared to the random and greedy approaches, the ELPA has significantly higher performance, which stems from its ability to manage interdependencies efficiently. The complexity of the problem is very dependent on the number of nodes $|N|$, and especially the number of interdependent sets $|B|$. When $|B|$ is high, the performance of the ELPA is much higher than that of the greedy and random approaches, and when $|A|$ is high, the runtime is higher for all approaches. Finally, and most importantly, the WSA and significance test conducted in the study can always serve as a decision support tool to ease operation and understanding in both the day-to-day scheduling process and the long-term strategic decision process.

Nonetheless, there exist several limitations to the research. Some assumptions could be relaxed to reflect more tangible insights. The price is assumed to remain uniform, which is inconsistent with commercial EOS imaging. In reality, it depends on the total size of the area, quality specification, satellite type, and even the waiting time of customers. Therefore, one of the next challenges is to integrate the influence of such industrial practices into the scoring system. Additionally, behavioral outcome objectives are still difficult to accommodate through the proposed ELECTRE-III scoring model. Therefore, it would be interesting to introduce linear or non-linear extensions to the criterion threshold or to incorporate reference actions for assigning scores as the ELECTRE-Score method [61]. Lastly, utilizing the developed scenario generator and solver in EOSpython to provide analyses for the design of EOS constellations in terms of the expected results one can obtain from certain orbit selections, platform characterstics, sensor types, etc, is of particularly high interest.

DATA AVAILABILITY

The source codes for the proposed algorithm and scenario generator are publicly available at https://github.com/AlexVasegaard/EOS

CRediT AUTHORSHIP CONTRIBUTION STATEMENT

The concept was developed with rigorous discussion among all the authors. A.E.V. took care of the coding parts for all computational aspect with thorough supervision from S.S. and P.N. Through the process, M.P. guided and checked the results. All the authors are equally involved in manuscript preparation.

ACKNOWLEDGMENT

The authors declare no conflict of interest.

REFERENCES

[1] K. T. Malladi, S. Mitrovic-Minic, and A. P. Punnen, "Clustered maximum weight clique problem: Algorithms and empirical analysis," *Comput. Oper. Res.*, vol. 85, pp. 113–128, Sep. 2017.

[2] M. Lemaître, G. Verfaillie, F. Jouhaud, J.-M. Lachiver, and N. Bataille, "Selecting and scheduling observations of agile satellites," *Aerosp. Sci. Technol.*, vol. 6, no. 5, pp. 367–381, Sep. 2002.
[3] Union of Concerned Scientists. (Jan. 1, 2023). *UCS Satellite Database (Excel Format)*. Accessed: Jul. 5, 2022. [Online]. Available: https://www.ucsusa.org/media/11492
[4] H. Kim and Y.-K. Chang, "Optimal mission scheduling for hybrid synthetic aperture radar satellite constellation based on weighting factors," *Aerosp. Sci. Technol.*, vol. 107, Dec. 2020, Art. no. 106287.
[5] A. A. Salman, I. Ahmad, and M. G. H. Omran, "A metaheuristic algorithm to solve satellite broadcast scheduling problem," *Inf. Sci.*, vol. 322, pp. 72–91, Nov. 2015.
[6] G. Miller, D. Rosenthal, W. Cohen, and M. Johnston, "Expert systems tools for Hubble space telescope observation scheduling," *Telematics Informat.*, vol. 4, no. 4, pp. 301–311, Jan. 1987.
[7] A. E. Vasegaard, "Multi-criteria decision making in complex decision environments," Ph.d.-serien for Det Ingenior- og Naturvidenskabelige Fakultet, Aalborg Universitetsforlag, 2023. [Online]. Available: https://doi.org/10.54337/aau561817671
[8] J. Jang, J. Choi, H.-J. Bae, and I.-C. Choi, "Image collection planning for Korea multi-purpose Satellite-2," *Eur. J. Oper. Res.*, vol. 230, no. 1, pp. 190–199, Oct. 2013.
[9] X. Chu, Y. Chen, and L. Xing, "A branch and bound algorithm for agile Earth observation satellite scheduling," *Discrete Dyn. Nature Soc.*, vol. 2017, pp. 1–15, Aug. 2017.
[10] C. Araguz, E. Bou-Balust, and E. Alarcón, "Applying autonomy to distributed satellite systems: Trends, challenges, and future prospects," *Syst. Eng.*, vol. 21, no. 5, pp. 401–416, Sep. 2018.
[11] X. Wang, G. Wu, L. Xing, and W. Pedrycz, "Agile Earth observation satellite scheduling over 20 years: Formulations, methods, and future directions," *IEEE Syst. J.*, vol. 15, no. 3, pp. 3881–3892, Sep. 2021.
[12] J. Sanchis, M. Martinez, and X. Blasco, "Integrated multiobjective optimization and a priori preferences using genetic algorithms," *Inf. Sci.*, vol. 178, no. 4, pp. 931–951, Feb. 2008.
[13] P. Tangpattanakul, N. Jozefowiez, and P. Lopez, "A multi-objective local search heuristic for scheduling Earth observations taken by an agile satellite," *Eur. J. Oper. Res.*, vol. 245, no. 2, pp. 542–554, Sep. 2015.
[14] X. Niu, H. Tang, and L. Wu, "Satellite scheduling of large areal tasks for rapid response to natural disaster using a multi-objective genetic algorithm," *Int. J. Disaster Risk Reduction*, vol. 28, pp. 813–825, Jun. 2018.
[15] Q. Wu and J.-K. Hao, "A review on algorithms for maximum clique problems," *Eur. J. Oper. Res.*, vol. 242, no. 3, pp. 693–709, May 2015.
[16] P. Wang, G. Reinelt, P. Gao, and Y. Tan, "A model, a heuristic and a decision support system to solve the scheduling problem of an Earth observing satellite constellation," *Comput. Ind. Eng.*, vol. 61, no. 2, pp. 322–335, Sep. 2011.
[17] J. Wang, E. Demeulemeester, D. Qiu, and J. Liu, "Exact and inexact scheduling algorithms for multiple Earth observation satellites under uncertainties of clouds," *IEEE Systems J.*, vol. 13, no. 3, pp. 3556–3567, 2018.
[18] M. Barkaoui and J. Berger, "A new hybrid genetic algorithm for the collection scheduling problem for a satellite constellation," *J. Oper. Res. Soc.*, vol. 71, no. 9, pp. 1390–1410, Sep. 2020.
[19] S. Augenstein, "Optimal scheduling of Earth-imaging satellites with human collaboration via directed acyclic graphs," in *Proc. AAAI Spring Symp. Ser.*, 2014, pp. 11–16.
[20] N. Bianchessi, J.-F. Cordeau, J. Desrosiers, G. Laporte, and V. Raymond, "A heuristic for the multi-satellite, multi-orbit and multi-user management of Earth observation satellites," *Eur. J. Oper. Res.*, vol. 177, no. 2, pp. 750–762, Mar. 2007.
[21] M. Küçük and S. T. Yildiz, "A constraint programming approach for agile Earth observation satellite scheduling problem," in *Proc. 9th Int. Conf. Recent Adv. Space Technol. (RAST)*, Jun. 2019, pp. 613–617.
[22] M. Vasquez and J.-K. Hao, "A 'logic-constrained' knapsack formulation and a tabu algorithm for the daily photograph scheduling of an Earth observation satellite," *Comput. Optim. Appl.*, vol. 20, no. 2, pp. 137–157, 2001.
[23] S. Hosseinabadi, M. Ranjbar, S. Ramyar, and M. Amel-Monirian, "Scheduling a constellation of agile Earth observation satellites with preemption," *J. Quality Eng. Prod. Optim.*, vol. 2, no. 1, pp. 47–64, 2017.
[24] D. Habet, M. Vasquez, and Y. Vimont, "Bounding the optimum for the problem of scheduling the photographs of an agile Earth observing satellite," *Comput. Optim. Appl.*, vol. 47, no. 2, pp. 307–333, Oct. 2010.
[25] K. Cui, J. Xiang, and Y. Zhang, "Mission planning optimization of video satellite for ground multi-object staring imaging," *Adv. Space Res.*, vol. 61, no. 6, pp. 1476–1489, Mar. 2018.
[26] J.-F. Cordeau and G. Laporte, "Maximizing the value of an Earth observation satellite orbit," *J. Oper. Res. Soc.*, vol. 56, no. 8, pp. 962–968, Aug. 2005.
[27] N. G. Hall and M. J. Magazine, "Maximizing the value of a space mission," *Eur. J. Oper. Res.*, vol. 78, no. 2, pp. 224–241, Oct. 1994.
[28] A. E. Vasegaard, M. Picard, F. Hennart, P. Nielsen, and S. Saha, "Multi criteria decision making for the multi-satellite image acquisition scheduling problem," *Sensors*, vol. 20, no. 5, p. 1242, Feb. 2020.
[29] J. Cui and X. Zhang, "Application of a multi-satellite dynamic mission scheduling model based on mission priority in emergency response," *Sensors*, vol. 19, no. 6, p. 1430, Mar. 2019.
[30] S. Wang, L. Zhao, J. Cheng, J. Zhou, and Y. Wang, "Task scheduling and attitude planning for agile Earth observation satellite with intensive tasks," *Aerosp. Sci. Technol.*, vol. 90, pp. 23–33, Jul. 2019.
[31] L. He, X.-L. Liu, Y.-W. Chen, L.-N. Xing, and K. Liu, "Hierarchical scheduling for real-time agile satellite task scheduling in a dynamic environment," *Adv. Space Res.*, vol. 63, no. 2, pp. 897–912, Jan. 2019.
[32] S.-W. Baek, S.-M. Han, K.-R. Cho, D.-W. Lee, J.-S. Yang, P. M. Bainum, and H.-D. Kim, "Development of a scheduling algorithm and GUI for autonomous satellite missions," *Acta Astronautica*, vol. 68, nos. 7–8, pp. 1396–1402, Apr./May 2011.
[33] V. Gabrel and D. Vanderpooten, "Enumeration and interactive selection of efficient paths in a multiple criteria graph for scheduling an Earth observing satellite," *Eur. J. Oper. Res.*, vol. 139, no. 3, pp. 533–542, Jun. 2002.
[34] L. Li, H. Chen, J. Li, N. Jing, and M. Emmerich, "Preference-based evolutionary many-objective optimization for agile satellite mission planning," *IEEE Access*, vol. 6, pp. 40963–40978, 2018.
[35] K. Wu, D. Zhang, Z. Chen, J. Chen, and X. Shao, "Multi-type multi-objective imaging scheduling method based on improved NSGA-III for satellite formation system," *Adv. Space Res.*, vol. 63, no. 8, pp. 2551–2565, Apr. 2019.
[36] Astrium. *Spot 6, Spot 7—Technical Sheet*. Accessed: Oct. 26, 2022. [Online]. Available: http://www.astrium-geo.com/files/pmedia/edited/r18072_9_spot_6_technical_sheet.pdf
[37] K. Govindan and M. B. Jepsen, "ELECTRE: A comprehensive literature review on methodologies and applications," *Eur. J. Oper. Res.*, vol. 250, no. 1, pp. 1–29, 2016.
[38] M. Petrović, N. Bojković, I. Anić, M. Stamenković, and S. P. Tarle, "An ELECTRE-based decision aid tool for stepwise benchmarking: An application over EU digital agenda targets," *Decis. Support Syst.*, vol. 59, pp. 230–241, Mar. 2014.
[39] Y. Liu, S. Zhang, and H. Hu, "A conflict avoidance algorithm for space-based collaborative stereo observation mission scheduling of space debris," *Adv. Space Res.*, vol. 70, no. 8, pp. 2302–2314, Oct. 2022.
[40] F. Perea, R. Vazquez, and J. Galan-Viogue, "Swath-acquisition planning in multiple-satellite missions: An exact and heuristic approach," *IEEE Trans. Aerosp. Electron. Syst.*, vol. 51, no. 3, pp. 1717–1725, Jul. 2015.
[41] Y. Wang, S. M. Minic, R. Leitch, and A. P. Punnen, "A GRASP for next generation sapphire image acquisition scheduling," *Int. J. Aerosp. Eng.*, vol. 2016, pp. 1–7, Sep. 2016.
[42] E. Bensana, G. Verfaillie, J. C. Agnese, N. Bataille, and D. Blumstein, "Exact and inexact methods for daily management of Earth observation satellite," *Space Mission Oper. Ground Data Syst.*, vol. 394, p. 507, Nov. 1996.
[43] R. Xu, H. Chen, X. Liang, and H. Wang, "Priority-based constructive algorithms for scheduling agile Earth observation satellites with total priority maximization," *Expert Syst. Appl.*, vol. 51, pp. 195–206, Jun. 2016.
[44] C. G. Valicka, D. Garcia, A. Staid, J.-P. Watson, G. Hackebeil, S. Rathinam, and L. Ntaimo, "Mixed-integer programming models for optimal constellation scheduling given cloud cover uncertainty," *Eur. J. Oper. Res.*, vol. 275, no. 2, pp. 431–445, Jun. 2019.
[45] M. Khan, "Longest path in a directed acyclic graph (DAG)," CSE Algorithms, Brac Univ., Dhaka, Bangladesh, 2011. [Online]. Available: https://blogs.asarkar.com/assets/docs/algorithms-curated/Longest%20Path%20in%20a%20DAG%20-%20Khan.pdf
[46] B. Meindl and M. Templ, "Analysis of commercial and free and open source solvers for linear optimization problems," in *Proc. Eurostat Statist. Netherlands Project ESSnet Common Tools Harmonised Methodol. SDC SS*, vol. 20, 2012, pp. 1–14.

[47] M. S. Andersen, J. Dahl, and L. Vandenberghe, "CVXOPT: A Python package for convex optimization," *Astrophys. Source Code Library*, 2020, Art. no. ascl-2008.
[48] H. Jiang, C. M. Li, and F. Manya, "An exact algorithm for the maximum weight clique problem in large graphs," in *Proc. AAAI*, 2017, pp. 830–838.
[49] S. Saha, A. E. Vasegaard, I. Nielsen, A. Hapka, and H. Budzisz, "UAVs path planning under a bi-objective optimization framework for smart cities," *Electronics*, vol. 10, no. 10, p. 1193, May 2021.
[50] R. Lahdelma, J. Hokkanen, and P. Salminen, "SMAA—Stochastic multiobjective acceptability analysis," *Eur. J. Oper. Res.*, vol. 106, no. 1, pp. 137–143, Apr. 1998.
[51] T. Tervonen and R. Lahdelma, "Implementing stochastic multicriteria acceptability analysis," *Eur. J. Oper. Res.*, vol. 178, no. 2, pp. 500–513, Apr. 2007.
[52] J. C. Arnold and J. S. Milton, *Introduction to Probability and Statistics: Principles and Applications for Engineering and the Computing Sciences*. New York, NY, USA: McGraw-Hill, 2003.
[53] M. Frank, "The Braess paradox," *Math. Program.*, vol. 20, no. 1, pp. 283–302, Dec. 1981.
[54] N. Banaeian, H. Mobli, B. Fahimnia, I. E. Nielsen, and M. Omid, "Green supplier selection using fuzzy group decision making methods: A case study from the agri-food industry," *Comput. Oper. Res.*, vol. 89, pp. 337–347, Jan. 2018.
[55] S. Chowdhury, A. Emelogu, M. Marufuzzaman, S. G. Nurre, and L. Bian, "Drones for disaster response and relief operations: A continuous approximation model," *Int. J. Prod. Econ.*, vol. 188, pp. 167–184, Jun. 2017.
[56] C. B. Pedersen, K. G. Nielsen, K. Rosenkrands, A. E. Vasegaard, P. Nielsen, and M. El Yafrani, "A GRASP-based approach for planning UAV-assisted search and rescue missions," *Sensors*, vol. 22, no. 1, p. 275, Dec. 2021.
[57] I. Sung and T. Lee, "Optimal allocation of emergency medical resources in a mass casualty incident: Patient prioritization by column generation," *Eur. J. Oper. Res.*, vol. 252, no. 2, pp. 623–634, Jul. 2016.
[58] W.-H. Feng, Z. Lou, N. Kong, and H. Wan, "A multiobjective stochastic genetic algorithm for the Pareto-optimal prioritization scheme design of real-time healthcare resource allocation," *Oper. Res. Health Care*, vol. 15, pp. 32–42, Dec. 2017.
[59] M. Caramia and P. Dell'Olmo, *Multi-Objective Management in Freight Logistics*, Springer, 2008.
[60] C. Bai, B. Fahimnia, and J. Sarkis, "Sustainable transport fleet appraisal using a hybrid multi-objective decision making approach," *Ann. Oper. Res.*, vol. 250, no. 2, pp. 309–340, Mar. 2017.
[61] J. R. Figueira, S. Greco, and B. Roy, "Electre-score: A first outranking based method for scoring actions," *Eur. J. Oper. Res.*, vol. 297, no. 3, pp. 986–1005, Mar. 2022.
[62] B. Roy, "Classement et choix en présence de points de vue multiples," *Revue Française D'informatique Recherche Opérationnelle*, vol. 2, no. 8, pp. 57–75, 1968.

ALEX ELKJÆR VASEGAARD received the M.Sc. degree in mathematics and economics and the Ph.D. degree in operations research from Aalborg University (AAU), in 2019 and 2023, respectively. He is currently a Postdoctoral Fellow with the Operations Research Group, AAU. He has had semesters and research stays abroad with the Royal Melbourne Institute of Technology, in 2018, Seoul National University, in 2021, University of the Bundeswehr Munich (2021–2022), University of Moratuwa, in 2022, and Polytechnique Montreal, in 2022. His research is within multi-criteria decision making, with a focus of integrating decision preferences into the decision-making process. The complex decision environments of interests include the problems of UAV routing and satellite scheduling.

MATHIEU PICARD received the Ph.D. degree. He is currently a Senior Expert on Satellite Ground Functions with Airbus Defense and Space (Space Systems Inc.). He has his education with École Polytechnique and Télécom Paris. His expertise covers the analysis, design and development of ground segment functional chains for space systems, and for a broad range of missions: earth observation, telecommunication, and navigation. He has contributed significantly to the research fields within earth observation systems engineering and signal processing.

PETER NIELSEN received the Ph.D. (Eng.) degree. He is currently an Associate Professor with the Department of Materials and Production. He is also a leading Expert on autonomous decision-making for large-scale cyber-physical systems and has published more than 150 scientific publications, including more than 40 journal articles in such prestigious journals, such as *Omega*, *International Journal of Information Management*, and *Journal of Cleaner Production*. He is also the Head of the Operations Research Group, Department of Materials and Production, and a member of numerous editorial boards. Since 2016, he has been leading more than ten larger research projects on AI with partners from Europe and Asia.

SUBRATA SAHA received the Ph.D. degree. He is a Professor with the University of Engineering and Management, Kolkata, India. He held an Assistant Professor position with the Department of Materials and Production, Aalborg University, Denmark. He was a Postdoctoral Research Fellow with the Department of Industrial Engineering, Seoul National University, South Korea, and an Assistant Professor with the Institute of Engineering and Management, Kolkata. He is the author of 69 articles in the journals, such as *International Journal of Production Economics*, *Annals of Operations Research*, *International Journal of Production Research*, *Journal of Cleaner Production*, *Transportation Research Part E: Logistics and Transportation Review*, *Aquaculture Journal*, *Journal of Retailing and Consumer Services*, *Computers & Industrial Engineering*, *Central European Journal of Operations Research*, and *Journal of Advanced Research*. His research interests include supply chain and inventory management, maritime logistics, and satellite image acquisition problems.